Effect of Lipid Composition on the "Membrane Response" Induced by a Fusion Peptide†

Pavel E. Volynsky,‡ Anton A. Polyansky,‡,§ Nikolay A. Simakov,‡ Alexander S. Arseniev,‡ and Roman G. Efremov*,‡

M. M. Shemyakin and Yu. A. Ovchinnikov Institute of Bioorganic Chemistry, Russian Academy of Sciences, Moscow, 117997, Russia, and Department of Bioengineering, Biological Faculty, M. V. Lomonosov Moscow State University, Moscow 119992, Russia

Received July 25, 2005; Revised Manuscript Received September 9, 2005

ABSTRACT: To understand the initial stages of membrane destabilization induced by viral proteins, the factors important for binding of fusion peptides to cell membranes must be identified. In this study, effects of lipid composition on the mode of peptides' binding to membranes are explored via molecular dynamics (MD) simulations of the peptide E5, a water-soluble analogue of influenza hemagglutinin fusion peptide, in two full-atom hydrated lipid bilayers composed of dimyristoyl- and dipalmitoylphosphatidylcholine (DMPC and DPPC, respectively). The results show that, although the peptide has a common folding motif in both systems, it possesses different modes of binding. The peptide inserts obliquely into the DMPC membrane mainly with its N-terminal α helix, while in DPPC, the helix lies on the lipid/water interface, almost parallel to the membrane surface. The peptide seriously affects structural and dynamical parameters of surrounding lipids. Thus, it induces local thinning of both bilayers and disordering of acyl chains of lipids in close proximity to the binding site. The "membrane response" significantly depends upon lipid composition: distortions of DMPC bilayer are more pronounced than those in DPPC. Implications of the observed effects to molecular events on initial stages of membrane destabilization induced by fusion peptides are discussed.

Enveloped viruses enter cells by membrane fusion. They accomplish this task by the use of specific envelope glycoproteins or fusion proteins. Usually, attachment of a virion to the target cell is mediated by anchoring of such proteins on the membrane surface via their conservative fragments, so-called "fusion peptides" (FPs),[1] consisting of about 20 amino acid residues (see refs *1* and *2* for recent reviews). As a result, FPs insert into the host membrane, providing close contact between lipid bilayers of the virus and cell. Understanding the molecular events that occur in cell membranes upon binding and insertion of FPs represents an intriguing challenge. Apart from the fundamental importance, solving the problem is invaluable in biomedical applications destined to prevent virus entry into cells.

FP of Influenza A virus hemagglutinin (HA) is one of the most promising objects for such studies. A wealth of experimental works have investigated its membrane-lytic properties. In these studies, the wild-type peptide HA has been shown to induce fusion of phospholipid vesicles in a pH-dependent manner (*3*−*7*). Also, fusion and leakage activities have been reported for a number of HA analogues (*4*, *8*). In particular, the spatial structures of HA and its active water-soluble analogue, peptide E5, have been solved by NMR spectroscopy in detergent micelles (*7*, *9*). Both peptides peripherally bind on the membrane surface and insert into the hydrophobic medium with their amphiphilic N-terminal α helices, while the C-terminal parts are rather flexible. At the same time, retrieval of high-resolution structural information about such systems in experiments is seriously hampered by limitations of modern experimental techniques (e.g., *10*). The development of molecular modeling approaches would be indispensable in avoiding these problems. Such methods have begun to be widely used in studies of protein−membrane interactions (see refs *11*−*13* for recent reviews). For example, behavior of the peptide HA and its analogues was studied via Monte Carlo simulations in implicit membranes (*14*, *15*). It has been shown that, regardless of the integral amphiphilic characteristics common to all such peptides, only the fusion-active ones reveal a specific "tilted oblique-oriented" pattern of hydrophobicity on their surfaces and penetrate on a certain depth into the nonpolar membrane

† This work was supported by the program RAS MCB, the Russian Foundation for Basic Research (Grants 04-04-48875-a and 05-04-49283-à), and the Ministry of Science and Technology of the Russian Federation (Lead 05, Living systems: Integrated project 3/001). R.G.E. is grateful to the Russian Science Support Foundation for the grant awarded. The authors thank the GROMACS developers team for providing the GROMACS software. Access to computational facilities of the Joint Supercomputer Center (Moscow) is gratefully acknowledged.

* To whom correspondence should be addressed. E-mail: efremov@nmr.ru. Fax/Telephone: +7-095-336-2000.

‡ Russian Academy of Sciences.

§ M. V. Lomonosov Moscow State University.

[1] Abbreviations: FP, fusion peptide; HA, FP of Influenza A virus hemagglutinin; E5, a water-soluble analogue of HA; MD, molecular dynamics; DMPC, dimyristoyl phosphatidylcholine; POPC, palmitoyloleoyl phosphatidylcholine; DPPC, dipalmitoyl phosphatidylcholine; DPC, dodecylphosphocholine; RMSD, root-mean-square deviation; RMSF, root-mean-square fluctuation; MHP, molecular hydrophobicity potential.

10.1021/bi0514562 CCC: $30.25
Published on Web 10/14/2005

core (*14*). On the other hand, the aforementioned experimental and modeling results do not address the question about the "membrane response" induced by peptide insertion. One possible solution to the problem lies in the application of molecular dynamics (MD) simulations of FPs in full-atom hydrated lipid bilayers.

Such calculations have been carried out to investigate the conformation of FP HA in the dimyristoyl phosphatidylcholine (DMPC) bilayer (*16*), showing that the peptide binds on the water−membrane interface and adopts a kinked conformation. This agrees well with the NMR data (*7*). Moreover, the influence of HA on the bilayer structure was detected. In particular, it was found that the average hydrophobic thickness of the lipid phase near the N terminus of HA is reduced as compared to that in the pure bilayer. The peptide HA and a set of its fusogenic and nonfusogenic analogues were also investigated by MD simulations in the palmitoyloleyl phosphatidylcholine (POPC) bilayer (*17*), demonstrating that the N-terminal α helix of the active analogues of FP is buried into the membrane with its N terminus and forms an angle ∼30° with the bilayer surface. Decreasing the bilayer thickness and destabilization of acyl chains of lipids caused by FP were also observed.

Often, binding of proteins, peptides, and other membrane-active agents to lipid bilayers as well as their functional activity in the membrane-embedded state essentially depend upon the physicochemical characteristics of the membrane. Native membranes consist of different types of lipids, vary in length and saturation of their acyl chains, properties of their headgroups, etc. The aforementioned MD results provided for the first time a wealth of interesting microscopic details related to the behavior of the peptide HA in two different membranes. On the other hand, several important aspects of FP−membrane interactions were not addressed in these studies. Among them, one can outline the following: (i) What are the microscopic details of peptide and water interactions with lipid headgroups in membranes of different composition? (ii) Are there any correlations between three-dimensional (3D) hydrophobic properties of a peptide and a bilayer (3D hydrophobic match effects)? (iii) Is the far-out leaflet of a bilayer sensitive to peptide insertion? Obviously, answers to these questions may help to gain an additional insight into molecular mechanisms of FPs' action on cell membranes.

With this aim in view, in the present work, we carried out long-term MD simulations of the fusion-active peptide E5 in two full-atom hydrated lipid bilayers composed of DMPC and dipalmitoyl phosphatidylcholine (DPPC). Special attention was given to the atomic-level details of the mutual influence of the peptide and the membrane on their behavior. The lipids were chosen for the following reasons. (i) They have similar headgroups and possess minor differences in the length of their acyl chains (two CH_2 groups). (ii) Despite that, the corresponding bilayers demonstrate rather different physicochemical properties (*18*). Thus, being similar in a packing density (close values of surface area/lipid), the DMPC bilayer is thinner and reveals a larger coefficient of lateral diffusion (i.e., it is more "fluid") as compared to the DPPC one. Therefore, the specific features of peptide−membrane interactions (if any) should mainly be caused by structural and dynamic characteristics of these lipid−water systems and not by the chemical nature of their particular groups.

Table 1: Parameters of the Systems under Study and MD Simulation Protocols

system[a]	*T* (K)[b]	box (Å^3)[c]	time (ns)[d]
E5/water$_{7043}$/Na$^+_5$	305	60.0 × 60.0 × 60.0	15
DMPC$_{128}$/water$_{3303}$	325 (296.5)	61.8 × 61.8 × 62.7	30
DPPC$_{128}$/water$_{3955}$	325 (314.5)	61.0 × 61.9 × 72.5	20
DMPC$_{128}$/water$_{7219}$/E5/Na$^+_5$	325	61.8 × 61.8 × 95.0	30
DPPC$_{128}$/water$_{5188}$/E5/Na$^+_5$	325	61.3 × 61.8 × 83.1	20

[a] E5, the peptide E5 (sequence, GLFEAIAEFIEGGWEGLIEG); subscripts indicate the number of lipid or water molecules and Na^+ counterions in the system. [b] The simulation temperature (temperature of phase transition liquid crystal−gel is given in brackets). [c] Size of the simulation box (the last value is the size along the normal to the membrane plane). [d] Time length of unrestrained MD runs.

MATERIALS AND METHODS

Construction of the Simulation Systems and the Computational Protocols. All simulations were performed using the GROMACS 3.2.1 (*19*) package and the GROMOS87 force field (*20*) specially adopted for lipids (*21*). Topologies of the DPPC and DMPC molecules were downloaded from the website http://moose.bio.ucalgary.ca/index.php?page=Downloads. Simulations were carried out with a time step of 2 fs, with imposed 3D periodic boundary conditions, in the NPT ensemble with an isotropic pressure of 1 bar. A twin-range (12/20 Å) spherical cutoff function was used to truncate nonbonded interactions. Previously, it has been shown that the cutoff-based MD simulations of explicit bilayers may lead to serious computational artifacts only in a case of electrostatically heterogeneous systems such as charged lipids and counterions (*22*, *23*). In contrast, the cutoff functions perform well for zwitterionic lipid bilayers composed, e.g., of DPPC or DMPC. That is why, to save a CPU time, MD simulations in this work were carried out with the cutoff functions for electrostatic interactions. All components of the systems (e.g., water and lipids for "pure" bilayers) were coupled separately using the Berendsen thermostat (*24*) to a temperature bath with a coupling constant of 0.1 ps. The simulation temperatures (Table 1) were chosen to ensure the liquid crystalline phase of lipid bilayers. Other parameters of the calculations are presented in Table 1.

Starting configurations of both bilayers were generated in a similar way using a molecular editor. The bilayer models were then placed into rectangular boxes and solvated by SPC water (*25*) molecules (Table 1). The resulting systems were taken as the starting points for MD simulations. Afterward, the systems were subjected to energy relaxation via 5×10^4 steps of steepest descent minimization followed by heating from 5 K to the temperature of simulations during a 50-ps MD run. Then, the long-term collection MD runs were carried out. The final configurations of DPPC and DMPC bilayers obtained in these calculations were further used in MD simulations of their complexes with the peptide E5.

The starting conformation of the peptide E5 was that obtained by NMR spectroscopy in dodecylphosphocholine (DPC) micelles (*9*). Its coordinates were provided by Dr. P. V. Dubovskii. Selection of a reliable starting configuration

of a peptide is one the most serious problems in MD studies with lipid bilayers. However, when the micelle-bound NMR structure of a peptide is known (like in the case with E5), its choice as the initial conformation appears to be the most plausible one. In water simulations, the peptide was placed in the center of a rectangular box and solvated by SPC waters. Because at pH 7 the peptide has a negative charge of −5, five water molecules were replaced by Na^+ ions to render the system electrically neutral. Positions of the last ones were chosen to provide the most favorable electrostatic contacts with the ionizing groups of E5. This was done with the help of the *genion* utility supplied with the GROMACS package. The system E5/water was equilibrated using a procedure identical to that for the "pure" bilayers, followed by a 15-ns MD run.

In simulations of E5 with lipid bilayers, the starting systems were constructed as follows. First, the water molecules were removed from the equilibrated box, and the peptide was placed at a distance ∼10 Å from the bilayer interface, with its hydrophobic residues oriented toward the membrane and the hydrophilic ones facing the water phase. Next, the systems were solvated, and five counterions were added (see above). The system was then subjected to energy minimization and subsequent heating during 5 ps. Finally, 2-ns MD simulations were carried out with an external acceleration of 1.0 Å/ps^2 applied to the peptide atoms along the normal to the membrane plane. At this stage, a number of NMR-derived geometrical restraints were employed to preserve initial conformation of the peptide. This was done just to avoid significant structural changes in the NMR model before bringing the peptide close to the bilayer surface. The following parameters were analyzed: (i) the depth of peptide insertion into the membrane, (ii) the energies of peptide−membrane interactions, (iii) the secondary structure of the peptide, (iv) the root-mean-square deviations (RMSDs) of peptide conformations from the NMR structure, and (v) hydrogen bonding. The resulting states [revealing a strong peptide−membrane interaction and small deviation from the initial peptide conformation (RMSD < 1 Å)] were taken as the starting structures for subsequent unrestrained MD runs.

Analysis of MD Trajectories. Analysis of MD trajectories was performed using original software developed by the authors and utilities supplied with the GROMACS package. Energies of electrostatic and van der Waals interactions between various components of the systems were calculated using the *g-nbi* program, specially written for this. The following macroscopic parameters of the simulated systems were analyzed: the area/lipid molecule (A_L), the mean order parameter of acyl chains of lipids (S_{CD}), the distance between phosphorus atoms of different bilayer leaflets (D_{PP}), the root-mean-square fluctuations (RMSFs) of coordinates of the heavy or C_α atoms of the peptide for each residue near their average equilibrium positions, the position of the residues of the peptide relative to the membrane, the energies of interactions of peptide residues with the membrane, the density distributions of phosphorus atoms and water along the normal to the membrane plane, and the acyl chain order parameter profiles. All of these parameters were averaged over the equilibrium parts of corresponding MD trajectories (last 5 ns). Hydrophobic properties of the peptide were calculated and visualized using the molecular hydrophobicity potential (MHP) approach as described elsewhere (*26*).

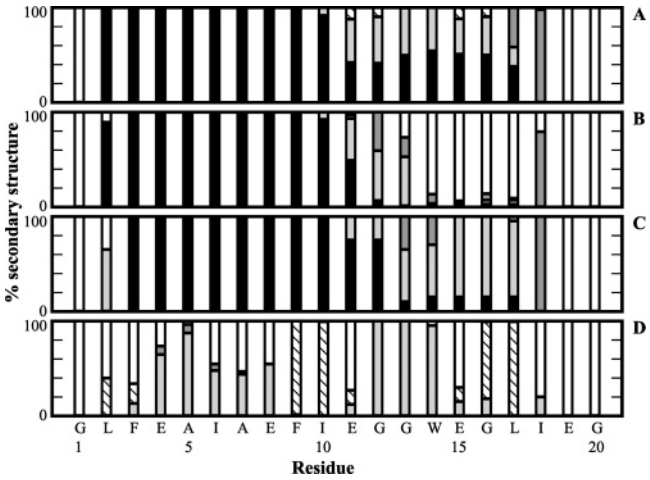

FIGURE 1: Secondary structure of the peptide E5. Relative occurrence of the residues of the peptide in different elements of secondary structure: black, α helix; light gray, β turn; dark gray, bend; white, random coil; and hatched, β sheet. The results obtained during the last 5 ns of MD simulation of E5 in the presence of DMPC (A) and DPPC (B) bilayers, respectively. (C) NMR-derived models of the peptide E5 in DPC micelles. (D) MD simulations of E5 in water.

RESULTS AND DISCUSSION

Lipid Bilayer Significantly Promotes the Secondary Structure of the FP. Analysis of MD data obtained for the peptide E5 in DPPC and DMPC bilayers clearly shows that the presence of the water−lipid interface considerably stabilizes α-helical conformation on the N terminus of the peptide. The time evolution of the secondary structure of membrane-bound E5 is shown in parts A and B of Figure 1. It is seen that in both bilayers the residues 2−10(11) form a stable α helix during all of the simulation time. These results agree well with the data derived from the analysis of a set of 20 3D structures of the peptide obtained by NMR spectroscopy in DPC micelles (Figure 1C). The only exception is that the helical segment in NMR models is shifted by one residue toward the C terminus. On the contrary, according to NMR and MD data, the C-terminal part of the peptide is rather more flexible. In the first case, it is mainly presented by β turns, although in a small number of NMR models the residues 13−17 form an α-helical conformation (Figure 1C). In the membrane-bound MD states, the conformation of the region 12−20 depends upon the bilayer. In the DMPC membrane, this part of E5 is more structured as compared to NMR data: residues 12−17 spend about 50% of the simulation time in α-helical conformation, and during practically all of the residual time, they adopt conformations stabilized by the intrapeptide hydrogen bonds (β turn or β bridge). In the DPPC membrane, these residues reveal no secondary structure.

In addition to the evolution of the secondary structure of E5 in time, one important issue is how flexible different peptide parts are on the water−membrane surface. Analysis of C_α RMSF values shows that in the presence of bilayers, the peptide has quite a rigid structure with RMSFs ∼ 0.5 Å (Figure 2B). The exceptions are provided by the C-terminal residue G20 in both membranes and by the residue G16 in

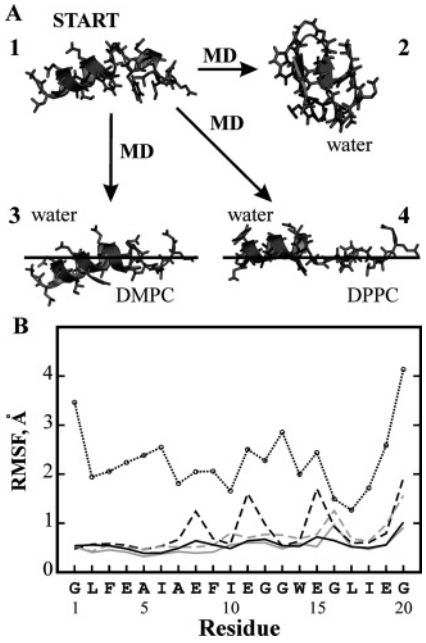

FIGURE 2: (A) Membrane-promoted stabilization of α-helical conformation. MD simulations of the FP E5 in full-atom lipid bilayers and water. (1) Starting structure. (2) Snapshot at the end of a 10-ns MD simulation in water. (3) Snapshot at the end of a 25-ns MD simulation in DMPC bilayer. (4) Snapshot at the end of a 15-ns MD simulation in DPPC bilayer. The α-helical region is given in a ribbon presentation. Lipid and water molecules are removed for clarity. The horizontal lines indicate the membrane interface, determined as a mean position of phosphorus atoms of lipids in the closest bilayer leaflet. (B) RMSF of the peptide heavy (- - -) and backbone (—) atoms for each residue, calculated during the last 5 ns of MD runs. The systems: E5/DPPC (gray), E5/DMPC (black), E5/water (heavy-atom RMSFs are shown with ···).

DPPC. Therefore, the peptide backbone in both bilayers is strongly conformationally restrained independently of its secondary structure (parts A and B of Figure 1): α-helical, *β*-turn, and coil regions of the peptide demonstrate equally low values of RMSF. This indicates that stabilization of a peptide on the membrane surface may be reached not only because of the formation of intramolecular hydrogen bonds (as in α helix and *β* turn), but it can also be induced by strong contacts of a completely or partly disordered peptide with the water−lipid interface. At the same time, unlike the DPPC membrane, the charged residues E8, E11, and E15 in DMPC reveal high RMSFs for heavy atoms. Therefore, the lability of these glutamic acids in DMPC is related to the behavior of their side chains. (Obviously, the lability of G16 in DPPC and G20 in both systems may be caused only by movements of their backbone atoms.) Possible reasons for such an unexpectedly high difference in mobility of side chains of residues E8, E11, and E15 in DMPC will be discussed later.

To assess the influence of the membrane on the structure and dynamics of the FP, these MD simulations were also carried out in aqueous solution. The results show that behavior of the peptide in water and in the presence of membrane differs dramatically. Thus, after 8-ns MD in water, the peptide completely loses its initial α-helical structure and adopts a tightly packed conformation (the values of accessible surface area are 1200 Å^2 in water and 1300−1350 Å^2 on the interface), where only a few residues are involved in the formation of the secondary structure elements (Figure 1D). This is pictorially illustrated by RMSD values between the starting structure and MD conformers obtained in water and in two bilayers. In aqueous solution, the RMSDs calculated over the heavy atoms of the peptide reach 8 Å at the end of the simulations, while on the water−lipid interface, they are less than 4 Å (data not shown). The high degree of conformational heterogeneity of the amphiphilic peptide in water is also confirmed by analysis of the corresponding heavy-atom RMSF values. As seen in Figure 2B, they are considerably higher than those obtained for the membrane-bound states. The instability of the α-helical conformation in water has two primary causes. First, because of the prominent amphiphilic character of the helix, a number of apolar side chains are exposed to a highly polar water environment. This significantly increases the free energy of the system and, therefore, destabilizes it. In the result, the peptide tends to change the conformation by distorting the rodlike helix and shielding the hydrophobic side chains from water. Second, water molecules compete with the backbone amides and carbonyls for hydrogen bonds, thus leading to a break of the corresponding intramolecular hydrogen bonds, which maintain the α-helical structure of E5.

To summarize, we can conclude that, unlike the aqueous solution, the water−membrane interface significantly promotes structuring of the anchored amphiphilic peptide. As discussed later, this facilitates its insertion into the lipid bilayer. Such effects are well-known from experiments (*27*). In addition, in the membrane-bound form, the peptide is highly conformationally constrained as compared to its water-soluble state. The lipid composition of the membrane does affect the structural and dynamic characteristics of the FP; overall, it is more structured in the more "fluid" (DMPC) membrane. Also, being adsorbed on the DMPC bilayer, the peptide reveals high flexibility of side chains of several negatively charged residues. In the next section, the following issues are addressed. What are the main factors determining peptide−membrane interactions? How does the binding proceed on the atomic level? Does the mode of membrane insertion depend upon the properties of lipid bilayers?

Modes of Peptide Insertion into Lipid Bilayers. MD simulations show that the peptide forms stable complexes with both lipid bilayers. It penetrates into the membranes via the N-terminal α helix, while the C-terminal fragment stays adsorbed on the bilayer surface (Figure 2A). Detailed characteristics of the binding are presented in Figure 3. First, let us consider the behavior of E5 in the DMPC membrane. As seen in Figure 3A, the peptide inserts into this bilayer with one side of its α helix (residues 1−3, 5−6, and 9−10) and with hydrophobic residues W14, L17, and I18. Among the C_α atoms, the maximal penetration depth (∼3−4 Å) is observed for residue L2 (Figure 3A). (The depth of insertion of a given residue corresponds to the average distance between its C_α atom and the center of the water−lipid interface defined as a mean *z* coordinate of phosphorus atoms.) During MD, the angle of insertion of the helix changes from ∼0° (starting conformation) to ∼40° (10−14 ns of MD) and then to ∼20° (after 17 ns of MD) (Figure 3B). (Hereinafter, the term "angle of insertion" indicates the angle between the helix axis and the membrane plane.) Therefore, the insertion is not a straightforward process; the peptide is "looking for" the optimal mode of membrane binding before being stabilized on the interface. This is

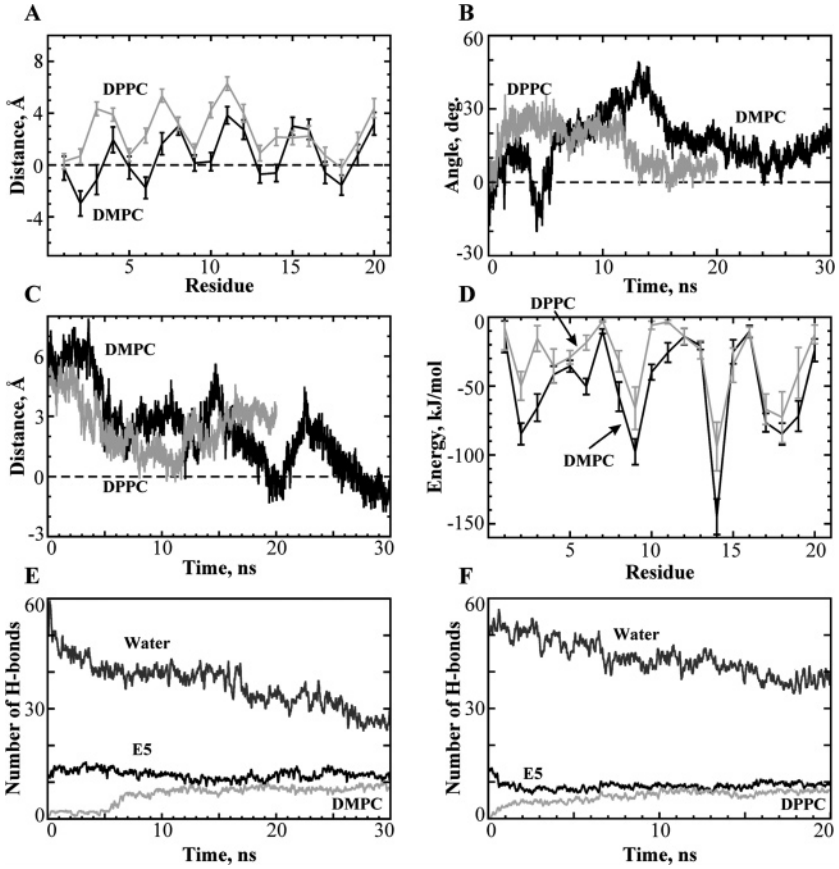

FIGURE 3: Interaction of the peptide E5 with DMPC (black) and DPPC (gray) bilayers. (A) Depth of insertion of the residues of the peptide into the membranes. The distance between C_α atoms of E5 and the center of the water−lipid interface (calculated as a mean *z* coordinate of phosphorus atoms). MD data are averaged over the last 5 ns of simulations. (B) Time evolution of the angle between the helix axis (calculated between residues 2 and 11) and the bilayer plane. (C) Distance between the center of mass of α helix 2−11 and the center of the upper bilayer leaflet. (D) Energies of peptide−membrane van der Waals interactions for each residue. MD data are averaged over the last 5 ns of simulations. (E and F) Number of hydrogen bonds between the peptide and different constituents of hydrated E5/DMPC (E) and E5/DPPC (F) bilayers. Data for E5, lipids, and water are shown with black, light-, and dark-gray lines, respectively.

accompanied by immersion of the helix into the interfacial region of the closest leaflet of the bilayer: the geometrical center of the helix reaches approximately the middle of the headgroups region after 17 ns of MD (Figure 3C). (Hereinafter this leaflet is called "upper", while the other one is referred to as "lower".) At the end of the simulation, the surface area of the peptide−membrane contact is about 1100 Å^2. A comparison of the MD results obtained for the peptide E5 in DMPC and DPPC membranes shows that the geometry of binding is sensitive to the bilayer properties. Thus, despite a similar tendency to insert into the DPPC membrane with the N-terminal helix, the peptide does not protrude into the lipid−water interface as deeply as in a case of DMPC (parts A and C of Figure 3). It remains considerably solvated by water and lies approximately parallel to the membrane plane (Figure 3B). The contact area between the peptide and the DPPC bilayer is considerably smaller, ∼900 Å^2. The mode of peptide binding to the hydrated DMPC bilayer agrees well with the experimental (*9*, *7*, *28*) and computational (*14*, *16*, *17*) data available for this and homologous FPs. Thus, the tilt angles measured in experiments are between 25° and 38°. It is also interesting to compare our results with those obtained for homologous FPs via MD simulations in full-atom hydrated lipid bilayers. Recently, Vaccaro et al. (*17*) reported such data for H3 influenza hemagglutinin FP and several its analogues in a relatively "loose" POPC bilayer. FPs studied in that work equilibrated their tilt angles to values of ∼30°. Not surprisingly, these peptides insert deeply into the POPC membrane; the maximal penetration depth for C_α atoms is ∼9 Å.

Apart from the analysis of geometrical parameters of insertion, the strength of peptide−membrane contacts in both bilayers was also assessed through calculations of the energies of nonbonded interactions of its residues with the environment. In the presence of the membranes, an essential gain in van der Waals energy (E_{vdW}) was observed (data not shown). On the contrary, the total energies of electrostatic interactions of the residues of the peptide with the environment (E_{elec}) remained practically invariable, although in DMPC, they were somewhat lower for the residues E11 and E15 (Figure 4). The strongest electrostatic interactions with the medium were detected for the charged residues (E4, E8, E11, E15, and E19), as well as for both termini. Also, in water, all of the negatively charged groups revealed close values of E_{elec}, while in the membrane, contributions of the N-terminal residues were relatively smaller. Such effects are especially pronounced for the system E5/DMPC. This is explained by insertion of the N-terminal helix of E5 into the hydrophobic membrane core, accompanied by movement of the peptide-charged groups away from the polar phase of the system.

The bilayer composition seriously affects the values of E_{elec} for individual residues. The first difference appears in the interaction of the N-terminal amino group with the

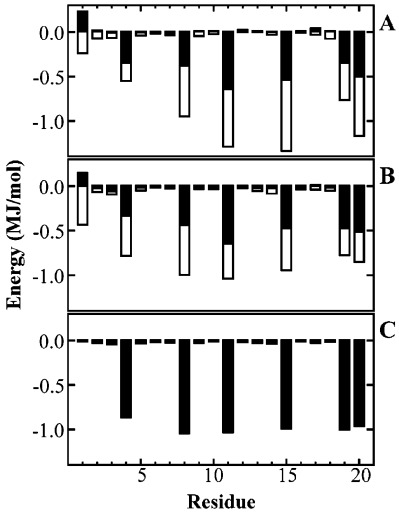

FIGURE 4: Energies of electrostatic interactions of the peptide E5 with the environment. MD data averaged over the last 5 ns of simulations. (A) DMPC/E5. (B) DPPC/E5. (C) E5/water. The contributions of water and lipid molecules are indicated with black and white bars, respectively.

environment: being almost negligible in DMPC (the values of E_{elec} describing contacts with lipids and water have opposite signs), in DPPC, the NH_3^+ group is accommodated in a favorable lipid environment (negative values of E_{elec}). For E5 in the DPPC bilayer, the contributions of lipids and water molecules into E_{elec} are quite similar. In contrast, in a case of the E5/DMPC system, the role of electrostatic interactions between the peptide and the polar headgroups of lipids (mainly cholines) becomes more important, especially for residues E11, E15, and E19 and for the C-terminal G20. This is caused by two reasons: (i) deeper insertion of E5 into the DMPC bilayer as compared with the DPPC one (Figure 3A), and (ii) protruding of some lipid molecules around the binding site into the water phase (Figure 5A). These lipids have favorable contacts with side chains of glutamic acids of the peptide. On the contrary, upon the peptide insertion, the DPPC bilayer retains its integrity well. In this case, side chains of Glu residues lie above the membrane surface and are rather less accessible to lipids (Figure 5B). We assume that the high flexibility (RMSF values, Figure 2B) of side chains of E8, E11, and E15 in DMPC is explained by their strong contacts with individual lipid molecules "plucked" from the bilayer into the water phase, while in the DPPC membrane, the lipids are much more structured, keeping their positions inside the bilayer.

Average values of peptide−lipid E_{vdW} are shown in Figure 3D. Here, the E_{vdW} profiles obtained for E5 in DMPC and DPPC membranes resemble each other, although the total value of E_{vdW} in the first case is significantly smaller. Also, some differences exist on the N terminus. Thus, the most favorable van der Waals contacts with the DMPC molecules are observed along almost the whole peptide length, for residues L2, F3, E4, A5, I6, E8, F9, I10, W14, L17, I18, and E19. In the DPPC membrane, such interactions are rather weaker; only residues L2, F9, W14, L17, I18, and E19 reveal low values of E_{vdW}.

How significant is the role of hydrogen bonding in peptide insertion? To answer this question, we performed an analysis of different types of hydrogen bonds during MD simulations of E5 in both bilayers. It was concluded that the time-

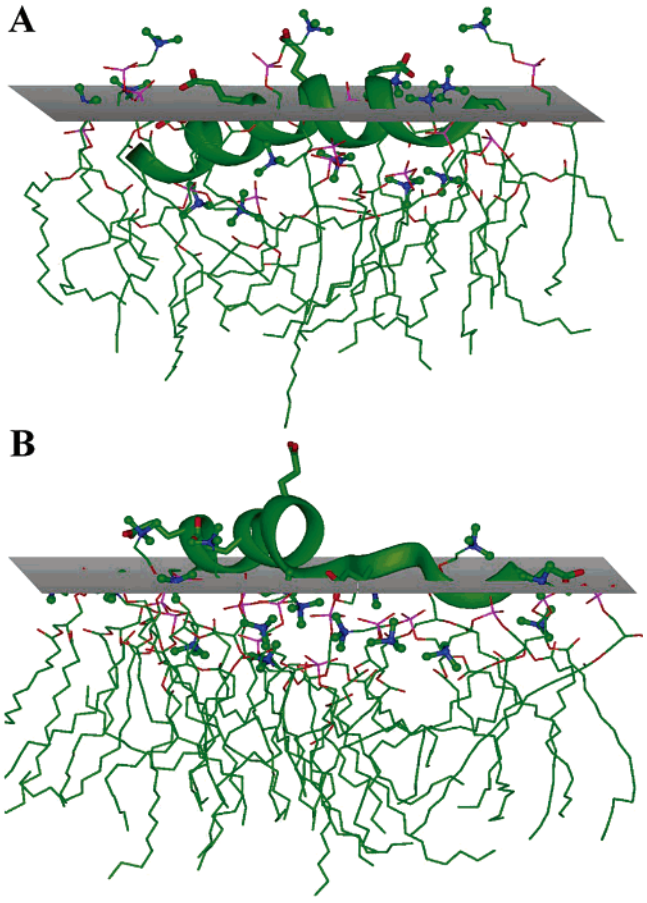

FIGURE 5: Mode of binding of the peptide E5 to DMPC (A) and DPPC (B) bilayers. Results of MD simulations. The peptide is given in a ribbon presentation, and side chains of glutamic acids are drawn with sticks. The water−lipid interface (calculated as a mean z coordinate of phosphorus atoms) is schematically shown with a gray-hatched plane. Water molecules are removed for clarity. Neighboring lipid molecules are indicated, and their choline groups are given in ball-and-stick presentation.

dependent redistribution of hydrogen bonds between the peptide and other components of the systems is quite similar. The number of intrapeptide and peptide−water hydrogen bonds decreases from 12 to 13 and 55 to 10−12 and 30−40, respectively, and 8−10 additional peptide−membrane hydrogen bonds appear (parts E and F of Figure 3). Decreasing the number of hydrogen bonds with water is caused mainly by screening of COO^- groups from the solvent, via choline groups of lipids. Also, deep penetration of some peptide residues into the membrane interface complicates involvement of their carbonyls in hydrogen bonds with other peptide groups and water. This was observed for residues E8, W14, L17, I18, and E19 in the DMPC bilayer and for G13, L17, and E19 in the DPPC bilayer. All backbone amide groups of the peptide participate in hydrogen bonding, although depending upon the studied system, the nature of these bonds differs. Thus, in water simulations, such bonds were mainly formed with solvent molecules, whereas in the presence of membranes, they were formed either with CO groups of the peptide (in the α-helical region) or with phosphate groups of lipids. In the E5/DMPC complex, stable peptide−lipid hydrogen bonds were observed for residues G1−E3, G12, and I18−E19, while in the DPPC bilayer, such bonds were found only on the termini of the peptide, for residues G1, L2, and L17−E19, respectively.

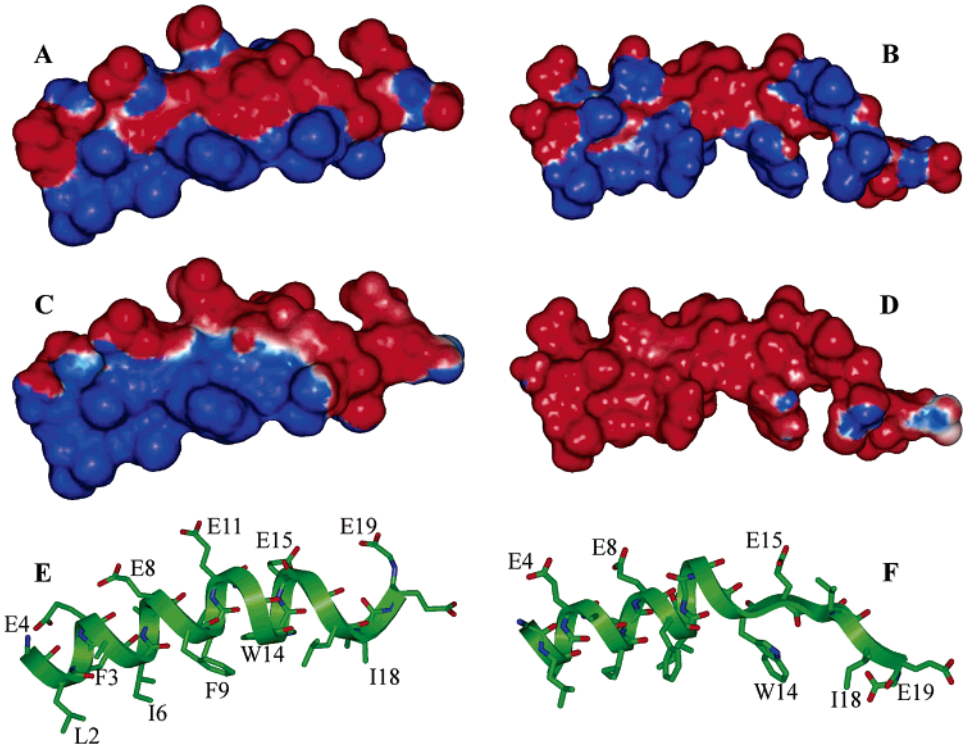

FIGURE 6: Spatial hydrophobic properties of the peptide surface. The peptide bound to DMPC (A, C, and E) and DPPC (B, D, and F) bilayers. The peptide surface is colored according to the values of molecular hydrophobicity potential (MHP) created in the surface points either by the atoms of E5 (A and B) or by surrounding lipids (C and D). Ribbon representations of the corresponding peptide structures are also shown (E and F). Hydrophobic (high MHP) and hydrophilic (low MHP) surface regions are shown in blue and red, respectively. Residues revealing strong interactions with lipids are marked.

Peptide−Membrane Binding: Complementarity of the 3D Hydrophobic Properties. It is well-established that binding of peptides on the water−membrane surface, as well as their insertion into the nonpolar core of lipid bilayers, is often mediated by hydrophobic interactions (*29*). Such systems reveal the prominent dominance of hydrophobic/hydrophobic and hydrophilic/hydrophilic contacts, while the hydrophobic/hydrophilic ones are too energetically costly to be frequently observed. For instance, the so-called "hydrophobic match/mismatch" effect, which reflects the correspondence between the length of hydrophobic membrane-spanning regions of a peptide and the thickness of a nonpolar membrane layer, is considered to be one of the most important factors driving peptide−membrane association (see ref *30* for a review). To estimate the role of similar effects in binding of the FP E5 to model membranes, we carried out a detailed analysis of spatial hydrophobic properties of the peptide and the lipid bilayer in the vicinity of their closest contacts. The main objective here was to check whether the hydrophobic and hydrophilic patterns on the surfaces of the peptide and the bilayer complement each other or not. The term "complement" means that in the equilibrium membrane-bound states the hydrophobic and hydrophilic groups of E5 tend to fall into hydrophobic and hydrophilic lipid environments, respectively. Spatial distributions of hydrophobic/hydrophilic properties were calculated using the MHP approach (see ref *26* for details). The peptide surface was mapped according to the MHP created by its own atoms ($MHP_{peptide}$) and by neighboring atoms of lipids ($MHP_{bilayer}$). This was done for the representative low-energy conformers bound to DMPC and DPPC bilayers (Figure 6). Positive and negative values of MHP correspond to hydrophobic and hydrophilic surface regions, respectively. The following conclusions can be made. In the E5 bound to DPPC, the distribution of $MHP_{peptide}$ has two well-defined hydrophobic surface patterns: on the N-terminal helix and on the C-terminal tail. The first one represents a nonpolar stretch protruding the whole helix length and oriented parallel to its axis (parts A and B of Figure 6). It is formed by residues L2, F3, A5, I6, A7, F9, and I10. The second pattern is created by residues L17, I18, and (partially) E19. Residue W14 forms an individual hydrophobic zone on the surface of the peptide. In the DMPC-bound conformation, all of these hydrophobic zones form one integral pattern. It is seen (parts A, C, and E of Figure 6) that better complementarity of $MHP_{peptide}$ and $MHP_{bilayer}$ distributions is observed for the E5/DMPC complex relative to the E5/DPPC one (parts B, D, and F of Figure 6). In the E5/DMPC complex, all hydrophobic regions of the peptide contact the apolar interior of the membrane (residues L2, F3, A5, I6, F9, W14, I18, and E19; Figure 6C), while in the second one, this is true only for residues W14, I18, and (partially) for E19. Better complementarity in the E5/DMPC complex is also observed for polar residues: in this case, hydrophilic DMPC headgroups contact the residues E4, E8, E11, G12, G13, E15, G16, and the C-terminal carboxyl group, while polar headgroups of DPPC interact only with E4, E8, G13, E15, G16, and terminal COO^- and NH_3^+ groups. In the DMPC bilayer, unfavorable hydrophobic/hydrophilic contacts are observed for residues G1, I10, and partially for G20. In the DPPC membrane, such contacts are realized for L2, F3, A5, I6, A7, F9, I10, L17, and partially for W14, I18, and G20. The hydrophobic residues that fall into the nonpolar lipid environment upon binding demonstrate the low energies of van der Waals

Table 2: Structural Characteristics of Pure Lipid Bilayers and Their Complexes with the Peptide E5

parameter[a]	DMPC exp[b]	MD	DMPC/E5 MD	DPPC exp	MD	DPPC/E5 MD
$\langle A_L \rangle$ (Å^2)	65.4	59.7 ± 0.1	58.9 ± 0.1	63.3	59.0 ± 0.1	58.7 ± 0.2
$\langle S_{CD} \rangle$	0.184	0.184 ± 0.019	0.189 ± 0.019	0.198	0.187 ± 0.018	0.191 ± 0.019
$\langle D_{PP} \rangle$ (Å)	33.8	35.24 ± 0.14	35.58 ± 0.19	38.2	38.90 ± 0.17	38.96 ± 0.19

[a] The calculated parameters are given as mean values ± standard deviations. Averaging was done for the last 5 ns of MD run (~500 MD conformers). A_L, area/lipid. S_{CD}, order parameters for acyl chains (experimental values are given for carbon atoms 1−8 of the acyl chain). D_{PP}, bilayer thickness, calculated as a distance between the peaks in the density distributions of phosphorus atoms. The experimental values of D_{PP} are estimated as $2(D_C + D_{H1})$, where D_C is the thickness of the hydrocarbon layer and D_{H1} is the partial thickness of the headgroup region (*36*). [b] Experimental results were obtained at $T = 323$ K. Data were taken from ref *37*.

interactions with the membrane, while the hydrophilic residues involved in favorable contacts participate in strong electrostatic interactions with the membrane. The aforementioned observations confirm the importance of the "hydrophobic match" effects in binding of the FP. We would like to outline that the results obtained using two independent methods lead to similar conclusions. Moreover, the MHP-mapping complements MD data. This method can be used for fast delineation of putative membrane-binding sites in FPs.

Detailed hydrophobic/hydrophilic properties of the peptide surface, along with the peptide−lipid hydrogen-bonding patterns may have grave consequences for the mode of peptide insertion. For example, many of FPs, including HA and its analogues, penetrate into membranes preferentially with their N termini (*31*, *32*). One reason for this is that their N-terminal parts are more hydrophobic. As follows from the results of current MHP analysis and our previous studies (*14*), in the membrane-bound states, these peptides expose most polar and nonpolar side chains to the water phase and to the membrane, respectively. Such a "hydrophobic match" effect considerably favors N-terminal insertion. Another support comes from the fact that burial of the N or C terminus would require dehydration of respectively NH or CO groups, which do not participate in intramolecular hydrogen bonds. However, dehydration of a carbonyl group is more energetically costly (*33*, *34*), thus promoting N-terminal insertion.

At the same time, there is a wealth of experimental (*35*) and simulation (*16*) data suggesting that in the membrane-bound form the N terminus of HA is protonated at both neutral and low pH. Therefore, at a first glance, burial of a charge +1 into apolar medium seems nonobvious from the energetic point of view. For instance, the log *P* value associated with partitioning of NH_3^+ group from water to octanol, a suitable mimic for the interfacial region, is ~ −1.75. At $T = 300$ K, the corresponding free-energy cost is about 2.4 kcal/mol. This calls for detailed inspection of interactions between the N-terminal residues of these peptides and the membrane lipids. Our MD results obtained for the peptide E5 in DMPC and DPPC bilayers clearly demonstrate that this is the residue G1, which possesses the strongest ability to form hydrogen bonds with lipids: during most of the simulation time, it simultaneously creates three such bonds. Each of them reduces the free energy at least by 2 kcal/mol. Therefore, the resulting gain in the free energy (~6 kcal/mol) compensates the energetic cost related to insertion of its charged NH_3^+ group into the hydrophobic membrane core. Such an assumption agrees well with those proposed earlier for some other peptides (*17*, *33*).

Destabilization of Lipid Bilayers Induced by the FP. To understand whether the membranes are sensitive to peptide insertion, structural and dynamical characteristics of both "pure" lipid bilayers, as well as their complexes with E5 were compared on the basis of the analysis of resulting MD trajectories (Table 2). We should emphasize that after the "switching-off" of the external force used to bring the peptide close to the membrane surface (see the Materials and Methods), characteristics of both bilayers were exactly the same as in their "peptide-free" states. This validates the applied computational protocol used at the initial 2-ns stage of MD; the detected effects of "membrane response" are caused by spontaneous (unrestrained) insertion of E5 into the interface and not by the external force. It is seen that, within the accuracy of the analysis, the presence of E5 has little effect on the average "global" equilibrium parameters calculated for the whole membranes: the surface area/lipid ($\langle A_L \rangle$), the membrane thickness ($\langle D_{PP} \rangle$), and the order parameters of acyl chains ($\langle S_{CD} \rangle$). On the other hand, there are prominent differences in distributions of some atomic groups of the lipid/water systems along the membrane normal. Thus, in the E5/DMPC complex, the increase of phosphorus density as compared with the "pure" bilayer is observed in the outer part of the lipid/water interface (Figure 7A). In this case, fluidity of the bilayer permits deep immersion of the peptide into the interface. This is accompanied by extrusion of a number of DMPC headgroups toward the water phase (Figure 5A). In contrast, in the E5/DPPC system, such a density growth is observed in the inner part of the interface; i.e., the peptide adsorbs from water on the bilayer surface and "pushes" several lipid headgroups toward the acyl chain region of the membrane. We should notice that, according to this criterion in both cases, there is practically no effect on the lower leaflets of the bilayers.

Dependent upon the bilayer content, important differences are also observed in distributions of water along the bilayer normal ($\rho_w(z)$). On the upper interface, the peptide induces different changes of the function $\rho_w(z)$ obtained for "pure" bilayers. As seen in Figure 7C, at $z > 0$, the differential curve $\Delta\rho_w(z) = \rho_w(z)_{E5/DPPC} - \rho_w(z)_{DPPC}$ has two negative (at 16 and 22 Å) and one positive (at 11 Å) peaks. The appearance of the negative peak at 22 Å is caused by exclusion of water molecules from the interfacial region by the bound peptide. This is confirmed by the fact that the density distribution of the peptide has a maximum at 21 Å (Figure 7B). The positive and negative peaks of $\Delta\rho_w(z)$ at 11 and 16 Å are explained by the peptide-induced displacement of a number of lipid headgroups with tightly bound water toward the nonpolar core of the bilayer. The characteristic length of such a displacement can be evaluated on the basis of the analysis

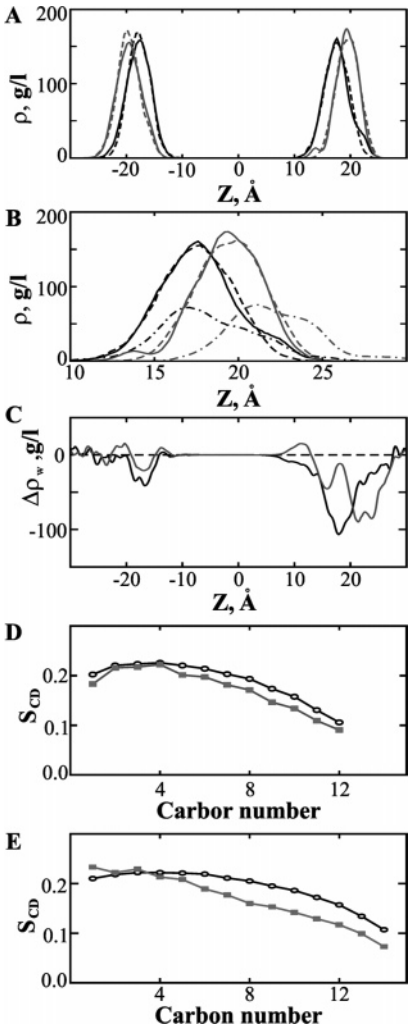

FIGURE 7: Peptide-induced "membrane response" (averaged over the last 5 ns of MD simulations). (A and B) Density distributions of phosphorus atoms along the membrane normal for the whole bilayers (A) and their upper leaflets (B). MD data in DMPC (black) and DPPC (gray) bilayers. (- - -) "Pure" bilayers. (—) Bilayers with bound peptide. (-•-) Peptide. (C) Changes in water distributions along the membrane normal [$\rho_w(z)$] caused by the peptide insertion. Differential curves [$\Delta\rho_w(z) = \rho_w(z)_{peptide/bilayer} - \rho_w(z)_{bilayer}$] for E5/DMPC and E5/DPPC systems are shown with black and gray lines, respectively. (D and E) Average order parameters (S_{CD}) for acyl chains of DMPC (D) and DPPC (E) bilayers. Data for all lipids (○) and for 10 lipid molecules revealing the strongest interactions with the peptide (■).

of density profiles for phosphorus atoms in the pure DPPC bilayer and in its complex with E5. As seen in Figure 7B, the last one reveals a shoulder separated by ~6 Å from the main maximum. This corresponds well to the distance between positive and negative peaks on the curve $\Delta\rho_w(z)$: 16 Å − 11 Å = 5 Å. Therefore, the aforementioned assumption about the origin of these peaks seems to be reasonable.

A somewhat different picture in water behavior is observed in the DMPC membrane. In the upper leaflet region, the function $\Delta\rho_w(z)$ reveals only one negative peak at 18 Å. Its integral intensity is close to that of the main negative peak (at 22 Å) in DPPC. As before, we attribute this peak to water molecules excluded from the interface by the adsorbed peptide [the density of the peptide in the E5/DMPC system has a maximum at 17 Å (Figure 7B)]. Because the left-hand part of the density profile for phosphorus atoms remains unchanged upon the peptide binding (Figure 7B), lipid headgroups are not "squeezed" into the acyl-chain region of DMPC; this bilayer is fluid enough to permit their "flow around" the inserted peptide. As a result, water molecules tightly coordinated with the phosphatidylcholine moieties do not change their distribution along the *z* axis. This explains the absence of additional peaks for the function $\Delta\rho_w(z)$. Interestingly, small (although nonnegligible) effects induced by the peptide are also observed on the lower leaflets of both bilayers: corresponding differential curves $\Delta\rho_w(z)$ reveal two positive (at −22 and −14 Å) and one negative (at −18 Å) peaks. We attribute these differences to local broadening of lower water−lipid interfaces.

Apart from the influence on the lipid headgroup regions, insertion of the peptide E5 affects the hydrophobic membrane core of both bilayers. This is illustrated by changes of order parameters (S_{CD}) of acyl chains of lipids. The values of S_{CD} obtained for the last 5 ns of MD and averaged over all lipid molecules in "pure" bilayers as well as in their complexes with E5 are presented in parts D and E of Figure 7. It is seen that the ordering of acyl chains in the entire bilayers practically does not change. One possible reason for this is that the influence of the peptide has a local character. To check this, the equilibrium values of S_{CD} were calculated for 10 lipid molecules, revealing the strongest interactions with the peptide. All of them are located in immediate proximity to the inserted fragment of E5. Indeed, as follows from parts D and E of Figure 7, binding of the peptide considerably destabilizes hydrocarbon tails of these lipids; this is reflected in the decrease of their S_{CD} values in both bilayers. Such a membrane perturbation effect is rather more pronounced in the more "fluid" DMPC bilayer. This coincides well with the conclusions made above based on analysis of other structural parameters of the two simulated systems. Comparing these S_{CD} profiles with those calculated on different time intervals during MD shows that the local disordering of lipids in the "shadow" of the peptide is caused by the insertion of E5 (data not presented). This tendency is observed in both lipid bilayers.

Additional insight into the microscopic picture of the "membrane response" may be gained via detailed analysis of in-plane distributions of various bilayer characteristics. Landscapes of the surfaces of the membranes are shown in parts A and B of Figure 8. It is seen that in each bilayer binding of the peptide is accompanied by formation of a "groove" on the upper leaflet surface. These grooves are located in the region of the peptide contact. They are deeper for the DMPC bilayer. In this case, lipid headgroups even form a peculiar "roof" above certain regions of the inserted peptide molecule, thus partly shielding it from aqueous solution (Figure 5A). This may explain fast decreasing of the number of peptide−water hydrogen bonds observed at the last stage of the corresponding MD run. In-plane distributions of the acyl-chain order parameters (S_{CD}) are shown in Figure 9. Areas of low S_{CD} are indicated with gray hatching. It is seen that the peptide causes disordering of lipids in the vicinity of the contact region. Such effects are more pronounced in DMPC, rather then in the DPPC bilayer (parts A and B of Figure 9). At the same time, within the errors associated with the technique, we cannot say whether the peptide influences on the ordering of lipids from lower leaflets of both membranes (parts C and D of Figure 9).

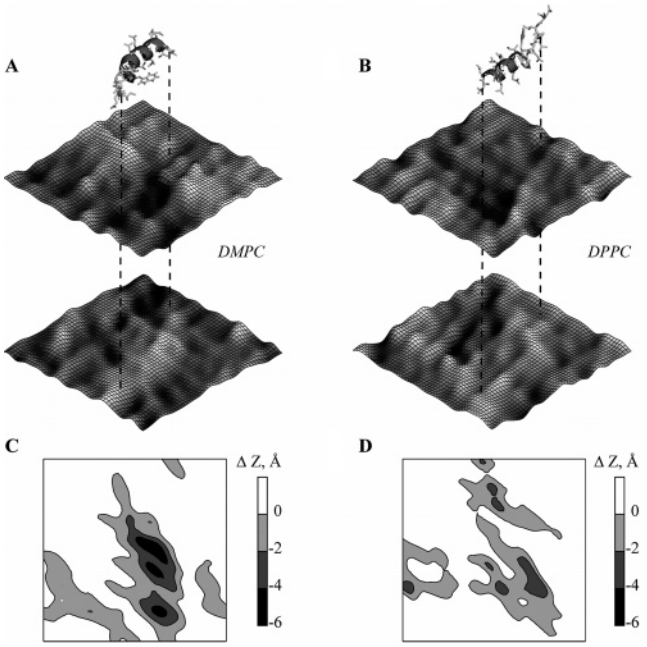

FIGURE 8: (A and B) Landscapes of the membrane surfaces for the last frames of MD simulations: (A) DMPC/E5 and (B) DPPC/E5. The peptide is shown in ribbon presentation. Its projection on the bilayer surface is indicated with vertical dashed lines. (C and D) Local thinning (ΔZ) of DMPC (C) and DPPC (D) bilayers induced by peptide binding. Two-dimensional contour maps obtained via subtraction of the landscapes for upper and lower leaflets of bilayers. The values of ΔZ indicate deviation from the thickness of pure bilayers. They are colored according to the scale shown near the corresponding map.

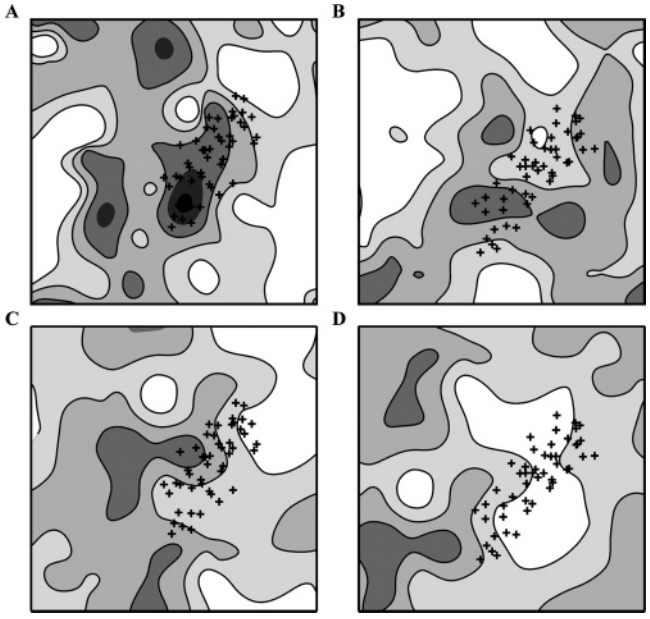

FIGURE 9: Local disordering of the DMPC (A and C) and DPPC (B and D) bilayers induced by the peptide binding. In-plane distribution of order parameters S_{CD} for the acyl chains of lipids. Ordered ($S_{CD} \sim 0.3$) and disordered ($S_{CD} \sim 0.0$) membrane regions are indicated with light- and dark-gray hatching, respectively. (A and B) and (C and D) correspond to upper and lower leaflets of lipid bilayers. Projections of the peptide atoms on the bilayer plane are shown by black crosses.

Three-dimensional maps of the surface landscapes (parts A and B of Figure 8) can be used to estimate the scale of the local thinning effects induced by the peptide in both bilayers. The differential 2D map (parts C and D of Figure 8) pictorially illustrates deviations of the membrane thickness from that obtained for the "pure" bilayer. Analysis of these data shows that in the "shadow" of the peptide the thickness of DMPC and DPPC bilayers is locally decreased up to 6 and 4 Å, respectively. Similar phenomena were also reported by Vaccaro et al. (*17*) based on the results of MD simulations of H3 influenza hemagglutinin FP in the POPC bilayer, although in that case, the effect was more pronounced: the authors observed a thinning of ~8 Å for the entire bilayer. When the unsaturated character of the POPC molecules was taken into account, the results of both studies seem to be consistent. However, we should note that Vaccaro et al. (*17*) did not check whether the membrane thinning has a local or global character.

It is significant that surfaces of both "pure" bilayers have overall roughness and ordering of acyl chains of lipids comparable to those in their complexes with the peptide (data not presented). Influence of the peptide consists of redistribution of the existing heterogeneities over the membrane surface; being spontaneously distributed in "pure" bilayers, in the presence of the peptide, they are mostly localized in the vicinity of the binding region.

Why do the simulation results for the E5/DMPC system fit better to the experimental observations than those for the E5/DPPC one? Previous differential scanning calorimetry studies (*38*) have demonstrated that phospholipid bilayers show increased intrinsic resistance to perturbation by the peptide with increasing length of their hydrocarbon chains. Qualitatively, this agrees well with our computational results. Moreover, as discussed above, the simulations can be used to propose possible molecular mechanisms of such effects. It will be recalled that the experimental structural information about FPs was mainly obtained in membrane mimics (DPC micelles). Therefore, it seems reasonable to assume that, unlike the DPPC, the macroscopic dynamic properties of the DMPC bilayer resemble the micellar environment better. Similar conclusion has been reached by Wong et al. (*39*) based on MD simulations of a fragment of the adrenocorticotropin hormone both in the DPC micelle and in the DMPC bilayer.

Structural Plasticity of the FP Is Mediated by Lipid Composition of the Membranes. Apart from the intuitively expected correlations between the physicochemical properties of lipid bilayers and the strength of their interactions with a given peptide ("the more fluid bilayer, the deeper insertion"), molecular modeling permits investigation of another important aspect of the peptide−membrane association. Namely, this is the problem of membrane-promoted accommodation of a peptide on the water−lipid interface. MD simulations started from the same conformation and orientation of the peptide with respect to the membrane surface clearly show that, depending upon the bilayer properties, the peptide adopts the optimal spatial structure and the geometry of insertion. Thus, the peptide E5 reveals strong helix-forming properties in its N-terminal part (residues 2−11). Being folded as an α helix, this fragment has a prominent amphiphilic character (parts A and B of Figure 6). Residues G12 and G13 provide an essential degree of conformational flexibility in the middle part of the peptide. Another important characteristic of all fusogenic analogues of HA is the presence of tryptophan in position 14. Such features of

the sequence help to understand different modes of accommodation of E5 on the two different membranes. In a case of the "fluid" bilayer (DMPC), the most efficient binding is achieved via tilted immersion of the hydrophobic side of the α helix into the nonpolar membrane core. Because of this, the residue W14 falls within the region of the polar headgroups and simultaneously interacts with the hydrocarbon tails of lipids. In turn, the lability of the C terminus makes possible its favorable contacts with the interface. Because of strong interactions of E5 with neighboring DMPC molecules, the hydrocarbon tails of these lipids are pulled out from the binding site. This causes disodering and thinning of the bilayer in the vicinity of the peptide binding.

A more "rigid" DPPC bilayer hampers deep insertion of the α-helical fragment of E5. As a consequence, the helix arranges on the bilayer surface parallel to the membrane plane. The helix−membrane contacts are not as favorable as in the previous case, although the residue W14 and the hydrophobic C-terminal part also reveal strong interactions with the membrane. Despite the very limited statistics (only two peptide/bilayer systems were studied here), we suppose that the effect of a peptide adaptation to a particular membrane may be common, at least for FPs homologous to HA. Such a kind of conformational plasticity is believed to be important for efficient action of FPs on cell membranes (see also refs *2*, *7*, and *17*). This is because the last ones often possess a high degree of structural heterogeneity, because of their domain organization, presence of bound proteins, peptides, and other molecules (including low-molecular-weight compounds).

CONCLUSIONS

The results of MD simulations of the FP E5 in hydrated DMPC and DPPC bilayers show that in both cases the behavior of the peptide has a number of common features. Thus, the presence of the membranes significantly stabilizes α-helical conformation of the peptide, especially in its N-terminal part (residues 2−11), while the C-terminal fragment is less ordered. The peptide forms stable complexes with lipid bilayers inserting into the hydrophobic membrane core with its hydrophobic residues and exposing the polar ones to water. The peptide is heavily involved in favorable electrostatic and van der Waals contacts with the membranes and also forms an extended network of hydrogen bonds with the headgroups of lipids. The interactions of hydrophobic residues with the membrane interior (acyl chains of lipids) are observed in both systems. Binding and insertion of the FP result in destabilization of lipid bilayers, although these effects have a local character; 10−15 only neighboring lipids significantly change their packing properties and dynamic behavior. On the other hand, several important parameters of peptide−membrane interaction seriously depend upon the lipid composition of bilayers. (i) The peptide binds stronger and penetrates deeper into the "fluid" DMPC membrane than into the relatively "rigid" DPPC one. The "membrane response" is more prominent in a case of the DMPC bilayer. This is reflected in larger local changes of the membrane thickness, width of the upper interfacial region, and disordering of acyl chains. (ii) Lipid composition also affects the deformation ability of the membrane surface. Thus, the groove on the upper monolayer of DMPC protrudes over the whole binding site of the peptide, while in the DPPC bilayer, it occurs only in the vicinity of the helix 2−11. (iii) Upon the peptide insertion, the DPPC bilayer retains its integrity well, although several lipids are "pushed" toward the acyl-chain region. In contrast, in the DMPC membrane, some lipid molecules around the binding site protrude into the water phase and strongly interact with glutamic acids of the peptide. (iv) Shortening of the hydrocarbon tail of lipids by two CH_2 groups (DMPC versus DPPC) may seriously affect the geometry of peptide binding. For example, the insertion angle for the N-terminal helix in DMPC bilayer is ∼20°, while in the DPPC membrane, it is arranged almost parallel to the membrane surface. The first result reproduces the mode of membrane binding known from experimental studies of fusogenic peptides well (*7*), and the second one is peculiar to their nonactive analogues (*14*, *17*). Therefore, computer simulations can help in delineation of direct relationships between the structural/dynamic properties of the membranes and the mode of peptide binding.

In the present work, we did not address the following important question: "What is the molecular mechanism of pH-dependent action of FPs?" The role of the media pH on the fusion activity of the peptide E5 was detected in experiments (*4*). It was proposed that the related mechanism involves protonation/deprotonation of the residue E11, thus changing hydrophobicity of the helical kink region (*9*). This can facilitate insertion of the entire α helix into the membrane and increase destabilization of lipid bilayer. However, such an assumption requires future validation, e.g., via MD simulations of lipid bilayers with the peptide E5 in different protonation states. This work is in progress now in our group.

We should stress that the membrane fusion phenomena induced by viral proteins are much more complex than the models elaborated with the aid of simplified systems, like FPs. Moreover, even in the last case, we are still far from understanding the detailed molecular mechanisms of the action of FPs on biomembranes. This is because too many factors determining peptide−membrane interactions have to be properly taken into account. Among them, there are the amino acid sequence of FPs and presence of specific sequence motifs, conformational flexibility of these peptides, details of their hydrophobic/hydrophilic organization (e.g., occurrence of the "tilted oblique-oriented patterns", complementarity of the 3D hydrophobic properties), media effects (e.g., pH, lipid composition of membranes, etc.), possible oligomerization processes, and so forth. Hopefully, the solution to the problem lies in systematic delineation of the relative contributions of such particular factors using independent experimental and theoretical techniques. These studies are currently being performed in many laboratories. For example, the role of pH and point mutations on the fusogenic activity of FPs may be proposed on the basis of a series of concordant results obtained by different research teams (see references in the Introduction). In the present work, an attempt was made to supplement the existing microscopic picture of FP−membrane interactions with the new data on the importance of lipid bilayers composition and their physicochemical properties. In particular, it was demonstrated that FPs may induce significant local perturbations of certain lipid bilayers, right up to extrusion of a number of lipid molecules into the water phase, like in a case of the DMPC membrane. Therefore, the efficiency of action of FPs on lipid membranes is a fine-tuning process

that depends not only upon the peptide, but is also determined by the "hospitality" of the membrane, by its ability to accommodate a given FP. Of course, further experimental and simulation structural studies are needed to decode the mystery of viral-mediated membrane fusion.

REFERENCES

1. Tamm, L. K., Crane J., and Kiessling, V. (2003) Membrane fusion: A structural perspective on the interplay of lipids and proteins, *Curr. Opin. Struct. Biol. 13*, 453−466.
2. Epand, R. M. (2003) Fusion peptides and the mechanism of viral fusion, *Biochim. Biophys. Acta 1614*, 116−121.
3. Lear, J. D., and DeGrado, W. F. (1987) Membrane binding and conformational properties of peptides representing the NH_2 terminus of influenza HA-2, *J. Biol. Chem. 262*, 6500−6505.
4. Murata, M., Sugahara, Y., Takahashi, S., and Ohnishi, S. (1987) pH-dependent membrane fusion activity of a synthetic twenty amino acid peptide with the same sequence as that of the hydrophobic segment of influenza virus hemagglutinin, *J. Biochem. 102*, 957−962.
5. Gray, C., and Tamm, L. K. (1998) pH-induced conformational changes of membrane-bound influenza hemagglutinin and its effect on target lipid bilayers, *Protein Sci. 7*, 2359−2373.
6. Korte, T., Epand, R. F., Epand, R. M., and Blumenthal, R. (2001) Role of the Glu residues of the influenza hemagglutinin fusion peptide in the pH dependence of fusion activity, *Virology 289*, 353−361.
7. Han, X., Bushweller, J. H., Cafiso, D. S., and Tamm, L. K. (2001) Membrane structure and fusion-triggering conformational change of the fusion domain from influenza hemagglutinin, *Nat. Struct. Biol. 8*, 715−720.
8. Epand, R. M., Epand, R. F., Martin, I., and Ruysschaert, J. M. (2001) Membrane interactions of mutated forms of the influenza fusion peptide, *Biochemistry 40*, 8800−8807.
9. Dubovskii, P. V., Li, H., Takahashi, S., Arseniev, A. S., and Akasaka, K. (2000) Structure of an analog of fusion peptide from hemagglutinin, *Protein Sci. 9*, 786−798.
10. Torres, J., Stevens, T. J., and Samso, M. (2003) Membrane proteins: The "Wild West" of structural biology, *Trends Biochem. Sci. 28*, 137−144.
11. Forrest, L. R., and Sansom, M. S. (2000) Membrane simulations: Bigger and better? *Curr. Opin. Struct. Biol. 10*, 174−181.
12. Efremov, R. G., Nolde, D. E., Konshina, A. G., Syrtcev, N. P., and Arseniev, A. S. (2004) Peptides and proteins in membranes: What can we learn via computer simulations? *Curr. Med. Chem. 11*, 2421−2442.
13. Ash, W. L., Zlomislic, M. R., Oloo, E. O., and Tieleman, D. P. (2004) Computer simulations of membrane proteins, *Biochim. Biophys. Acta 1666*, 158−189.
14. Efremov, R. G., Nolde, D. E., Volynsky, P. E., Chernyavsky, A. A., Dubovskii, P. V., and Arseniev, A. S. (1999) Factors important for fusogenic activity of peptides: Molecular modeling study of analogs of fusion peptide of influenza virus hemagglutinin, *FEBS Lett. 462*, 205−210.
15. Bechor, D., and Ben-Tal, N. (2001) Implicit solvent model studies of the interactions of the influenza hemagglutinin fusion peptide with lipid bilayers, *Biophys. J. 80*, 643−655.
16. Huang, Q., Chen, Ch.-L., and Herrmann, A. (2004) Bilayer conformation of fusion peptide of influenza virus hamgglutinin: A molecular dynamics study, *Biophys. J. 87*, 14−22.
17. Vaccaro, L., Cross, K. J., Kleinjung, J., Straus, S. K., Thomas, D. J., Wharton, S. A., Skehel, J. J., and Fraternali, F. (2005) Plasticity of influenza haemagglutinin fusion peptides and their interaction with lipid bilayers, *Biophys. J. 88*, 25−36.
18. Nagle J. F., and Tristram-Nagle, S. (2000) Lipid bilayer structure, *Curr. Opin. Struct. Biol. 10*, 474−480.
19. Lindahl, E., Hess, B., and van der Spoel, D. (2001) A package for molecular simulation and trajectory analysis, *J. Mol. Mod. 7*, 306−317.
20. van Gunsteren, W. F., and Berendsen, H. J. C. (1987) *Gromos-87 Manual*, Biomos BV, Nijenborgh 4, 9747 AG Groningen, The Netherlands.
21. Berger, O., Edholm, O., and Jahnig, F. (1997) Molecular dynamics simulations of a fluid bilayer of dipalmitoylphosphatidylcholine at full hydration, constant pressure, and constant temperature, *Biophys. J. 72*, 2002−2013.
22. Rog, T., Murzyn, K., and Pasenkiewicz-Gierula, M. (2003) Molecular dynamics simulations of charged and neutral lipid bilayers: Treatment of electrostatic interactions, *Acta Biochim. Pol. 50*, 789−798.
23. Polyansky, A. A., Volynsky, P. E., Nolde, D. E. Arseniev, A. S., and Efremov, R. G. (2005) Role of lipid charge in organization of water/lipid bilayer interface: Insights via computer simulations, *J. Phys. Chem. B 109*, 15052−15059.
24. Berendsen, H. J. C., Postma, J. P. M., DiNola, A., and Haak, J. R. (1984) Molecular dynamics with coupling to an external bath, *J. Chem. Phys. 81*, 3684−3690.
25. Berendsen, H. J. C., Postma, J. P. M., van Gunsteren, W. F., and Hermans, J. (1981) Interaction models for water in relation to protein hydration, in *Intermolecular Forces*; Pullman, B., Ed.; pp 331−342, Reidel, Dordrecht, The Netherlands.
26. Efremov, R. G., and Vergoten, G. (1995) Hydrophobic nature of membrane-spanning α-helical peptides as revealed by Monte Carlo simulations and molecular hydrophobicity potential analysis, *J. Phys. Chem. 99*, 10658−10666.
27. White, S. H., and Wimley, W. C. (1999) Membrane protein folding and stability: Physical principles, *Annu. Rev. Biophys. Biomol. Struct. 28*, 319−365.
28. Morris, K. F., Gao, X., and Wong, T. C. (2004) The interactions of the HIV gp41 fusion peptides with zwitterionic membrane mimics determined by NMR spectroscopy, *Biochim. Biophys. Acta 1667*, 67−81.
29. Killian, J. A. (1998) Hydrophobic mismatch between proteins and lipids in membranes, *Biochim. Biophys. Acta 1376*, 401−415.
30. Webb, R. J., East, J. M., Sharma, R. P., and Lee, A. G. (1998) Hydrophobic mismatch and the incorporation of peptides into lipid bilayers: A possible mechanism for retention in the Golgi, *Biochemistry 37*, 673−679.
31. Bechinger, B., Gierasch, L. M., Montal, M., Zaloff, M., and Opella, S. J. (1996) Orientations of helical peptides in membrane bilayers by solid-state NMR spectroscopy, *Solid State NMR Spectrosc. 7*, 185−192.
32. Brasseur, R., Pillot, T., Lins, L., Vandekerckhove, J., and Rosseneu, M. (1997) Peptides in membranes: Tipping the balance of membrane stability, *Trends Biochem. Sci. 22*, 167−171.
33. Chipot, C., and Pohorille, A. (1998) Folding and translocation of the undecamer of poly-L-leucine across the water−hexane interface. A molecular dynamics study, *J. Am. Chem. Soc. 120*, 11912−11924.
34. Ben-Tal, N., Ben-Shaul, A., Nicholls, A., and Honig, B. (1996) Free-energy determinants of α-helix insertion into lipid bilayers, *Biophys. J. 70*, 1803−1812.
35. Zhou, Z., Macosko, J. C., Hughes, D. W., Sayer, B. G., Hawes, J., and Epand, R. M. (2000) ^{15}N NMR study of the ionization properties of the influenza virus fusion peptide in zwitterionic phospholipid dispersions, *Biophys. J. 78*, 2418−2425.
36. Nagle, J. F., and Tristram-Nagle, S. (2000) Structure of lipid bilayers, *Biochim. Biophys. Acta 1469*, 159−195.
37. Petrache, H. I., Dodd, S. W., and Brown, M. F. (2000) Area per lipid and acyl length distributions in fluid phosphatidylcholines determined by ^2H NMR spectroscopy, *Biophys. J. 79*, 3172−3192.
38. Surewicz, W. K., and Epand, R. M. (1986) Phospholipid structure determines the effects of peptides on membranes. Differential scanning calorimetry studies with pentagastrin-related peptides, *Biochim. Biophys. Acta 856*, 290−300.
39. Wong, T. C., and Kamath, S. (2002) Molecular dynamics simulations of adrenocorticotropin (1−24) peptide in a solvated dodecylphosphocholine (DPC) micelle and in a dimyistoylphosphatidylcholine (DMPC) bilayer, *J. Biomol. Struct. Dyn. 20*, 39−57.

BI0514562